# SUBCELLULAR EXPRESSION OF AQUAPORIN-4 IN SUBSTANTIA NIGRA OF NORMAL AND MPTP TREATED MICE

AGNETE PRYDZ[a], KATJA STAHL[a], MAJA PUCHADES[a], NINA DAVARPANEH[a], MARIA NADEEM[a], OLE PETTER OTTERSEN[a], VIDAR GUNDERSEN[a, b], MAHMOOD AMIRY-MOGHADDAM[a*].

[a] *Division of Anatomy and Healthy Brain Ageing Center Reginal Research Network, Department of Molecular Medicine, Institute of Basic Medical Sciences, University of Oslo, PO box 1105, Blindern, 0317 Oslo, Norway*

[b] *Department of Neurology, Oslo University Hospital, Rikshospitalet, PO Box 4950 Nydalen, 0424 Oslo, Norway*

* Corresponding Author: Mahmood Amiry-Moghaddam, mahmo@medisin.uio.no

**Abstract**

Aquaporin-4 (AQP4) is the predominant water channel in mammalian CNS where it is localized at the perivascular astrocytic foot processes abutting brain microvessels. Several lines of evidence suggest that AQP4 is involved in important homeostatic functions and that mislocalization of the perivascular pool of AQP4 is implicated in several different brain disorders. A recent study suggests that the differential susceptibility of midbrain dopaminergic neurons to the parkinsonogenic toxin 1-methyl-4-phenyl-1,2,3,6-tetrahydropyridine (MPTP) depends on the expression of AQP4. Further, MRI studies of patients with Parkinson's disease (PD) point to an excessive water accumulation in the substantia nigra (SN). This prompted us to investigate the cellular and subcellular distribution of AQP4 in mouse SN using immunofluorescence and quantitative immunogold cytochemistry. Compared with neocortex, SN exhibits a higher concentration of AQP4. Specifically, judged by electron microscopic immunogold analysis, the perivascular density of AQP4 in SN exceeds by 70% the perivascular density of AQP4 in the neocortex. An even larger difference in AQP4 labeling was found for astrocytic processes in the neuropil. Treatment with MPTP further increased (by >30 %) the perivascular AQP4 density in SN, but also increased AQP4 labeling in the neocortex. Our data indicate that the perivascular AQP4 pool in SN is high in normal animals and even higher after treatment with MPTP. This would leave the SN more prone to water accumulation and supports the idea that AQP4 could be involved in the pathogenesis of PD.

**Keywords:** Aquaporin-4, astrocyte, MPTP, Parkinson's disease, immunogold histochemistry.
*Abbreviations:* Aquaporin-4 (AQP4), 1-methyl-4-phenyl-1,2,3,6-tetrahydropyridine (MPTP), Parkinson's disease (PD), substantia nigra (SN), substantia nigra pars compacta (SNpc), dopaminergic neuron (DA).

## INTRODUCTION

Parkinson's disease (PD) is the second most common neurodegenerative disorder in the Western hemisphere, characterized by progressive neuronal cell death predominantly of the dopaminergic neurons (DA) in substantia nigra pars compacta (SNpc) (Hirsch et al. 2013). More than 90% of all cases with PD have unknown etiology and the mechanisms underlying the selective loss of nigral DA neurons are not understood. Evidence is accumulating to suggest that astrocytes might play a role in the pathophysiology of PD (Mena and García De Yébenes 2008) and recent studies in animal models of PD have indicated an involvement of the astrocytic water channel aquaporin-4 (AQP4) (Fan et al. 2008; Sun et al. 2016; Yang et al. 2011; Zhang et al. 2016). Moreover, MRI studies of patients with PD have revealed an abnormal water accumulation in the SN (Ofori et al. 2015a). However, the cellular and subcellular expression of AQP4 in the SN is unknown, as is the expression level of AQP4 in the parkinsonian brain.

Studies of other brain regions have revealed that AQP4 is concentrated in astrocytic endfeet that encompass the blood-brain and brain-liquid interfaces (Nielsen et al. 1997) (Amiry-Moghaddam and Ottersen 2003; Rash et al. 1998). The polarized expression of AQP4 in astrocytes is crucial for homeostatic processes maintaining normal function, including water and potassium homeostasis (Nagelhus et al. 1999). Further, polarized expression of AQP4 has been shown to be important for cell migration (Saadoun et al. 2005) and possibly astrocytic $Ca^{2+}$ signaling (Thrane et al. 2011). Loss of the polarized expression of AQP4 has been shown in several pathological conditions, such as stroke (De Castro Ribeiro et al. 2006; Frydenlund et al. 2006), temporal lobe epilepsy (Alvestad et al. 2013) and Alzheimer's disease (Yang et al. 2011). Here we used immune-microscopy in healthy mice and mice treated with the parkinsonogenic toxin MPTP to ask whether the SN differs from other brain regions with respect to the expression of AQP4 and whether the expression of AQP4 in SN is sensitive to MPTP.

Our data indicate that astrocytes in the SN differ from those in neocortex by showing a higher level of AQP4, particularly in those endfoot membrane domains that mediate water exchange between brain and blood. Nine days after treatment with MPTP the AQP4 pool in these membrane domains has increased further, and more so than the AQP4 pools in other domains of the astrocyte membrane. AQP4 overexpression in specific astrocyte membrane domains may contribute to the water dyshomeostasis observed in patients with PD.

## EXPERIMENTAL PROCEDURES

### Animals

Male wild type C57BL/6 mice 8-12 weeks were used in this study. Experimental protocols were approved by the Institutional Animal Care and Use Committee and conform to National Institutes of Health guidelines for the care and use of animals.

### Tissue preparation

Untreated animals

Animals were anesthetized deeply with hypnorm dormicum (0.105 mg/kg) followed by intracardial perfusion. For light microscopy of untreated SN and neocortex, the animals (n=5) were perfusion-fixed with 4% formaldehyde (FA) in 0.1M phosphate buffer (PB) (Sigma-Aldrich, St. Louis, MO, USA) using pH-shift (Eilert-Olsen et al. 2012) starting with pH 6.0 for 5 minutes, then shifting to pH 10.5 for 10 minutes. The brains were dissected out and post-fixed overnight in 4% FA with pH 10.5. Animals used for electron microscopy (n=3) were perfusion-fixed with 4% FA and 0.1% glutaraldehyde (GA) in 0.1 PB (Sigma-Aldrich), and then post-fixed in the same solution overnight. All brains were stored in a 1:10 dilution of their respective fixative at 4°C until further preparations.

MPTP and saline treated animals

Mice were treated with either MPTP or saline, following an acute protocol as previously described (Puchades et al. 2013; Jackson-Lewis et al. 1995; Vernice and Serge 2007). One series of MPTP treated mice and controls was used for EM studies and another series was used for light microscopic immunohistochemistry. For EM experiments, male C57 BL/6 mice (n=5; 8 weeks of age; Taconic, Denmark) received MPTP-HCl free base (Sigma-Aldrich) in an acute paradigm (four injections subcutaneously at 2h intervals, 18 mg/kg for each

injection) (Vernice and Serge 2007). The control mice (n=5) received injections of saline (4 mL/kg). For light microscopic immunohistochemistry, male C57 BL/6 mice (n=4; 12 weeks of age; Taconic, Denmark) received MPTP-HCl free base (Sigma-Aldrich) in an acute paradigm (three subcutaneous injections of 15 mg/kg at 2 h intervals) The control mice (n=3) received injections of saline (4 mL/kg). The MPTP dosage was reduced in the second series in order to reduce the acute mortality associated with the higher MPTP concentration. Based on Jackson-Lewis et al (Jackson-Lewis et al. 1995) who showed that the degeneration of dopamine neurons started within the first day after MPTP treatment, reached a plateau at day 4, and was thereafter stable till day 28, , we chose a survival time of 9 days after the last MPTP injection. The choice of this time point is also in line with the recommendations of Vernice and Serge 2007 (Vernice and Serge 2007). From day 7 till day 28 TH-immunoreactivity can be used to determine accurately the number of living neurons in SNpc (Jackson-Lewis et al. 1995). Nine days after the last injection, both groups of animals were deeply anesthetized with pentobarbital (0.1mL/50g body weight) followed by transcardial perfusion of either 4% FA and 0.1% GA or 4% FA for 10 min and post-fixed *in situ* overnight (Puchades et al. 2013). Tissue samples from the 4% FA fixed brains were used for immunofluorescence analysis and samples from both fixatives were used for the immunogold analysis. The difference in the fixatives did not have any impact on the density of the immunogold labeling (data not shown). The brains were dissected out and either processed for electron microscopy or cut into 30 µm coronal sections using a Vibratome (Microm, Jacksonville, FL, USA) for immunohistochemistry and stored at 4ºC in 1/10 fixative until further preparations.

Immunofluorescence and confocal microscopy

The immunofluorescence labeling was performed as described previously (Yang et al. 2011). In brief, the sections were treated with 10% normal goat serum (NGS) and 1% bovine serum albumin (BSA) upon incubation with primary antibodies overnight in 3% NGS, 1% BSA, 0.5% Triton-X-100 and 0.05% sodium azide in 0.01M phosphate buffer saline (all chemicals from Sigma-Aldrich). Following washing, the sections were incubated with secondary antibodies, washed in PBS, and mounted with Prolong Gold Antifade Reagent with DAPI (Invitrogen, Norway). A complete list of the primary and secondary antibodies used in this study is presented in Table 1. Images were collected with a LSM 510 META Confocal Microscope (Zeiss, Jena, Germany) using a 40x oil objective. DAPI fluorescence was captured at 405 nm, Alexa 488 at 510 nm, Cy3 at 568 nm and Cy5 at 670 nm.

**Table 1** Antibodies

| Method | Primary antibody | Secondary antibody |
|---|---|---|
| Immunogold | AQP4, host: rabbit, Sigma-Aldrich, diluted 1:400 | Goat anti-rabbit 15 nm gold, Abcam, diluted 1:20 |
| Immunofluorescence | AQP4, host: rabbit, Sigma-Aldrich, diluted 1:400 | Cy3 donkey anti-rabbit, Jackson, diluted 1:500 |
| | TUJ1, host: mouse, Covance, diluted 1:1000 | Alexa 488 donkey anti-mouse, Invitrogen, diluted 1:500 |
| | TH, host mouse, Chemicon, diluted 1:1000 | Alexa 488 donkey anti-mouse, Invitrogen, diluted 1:500 |
| | GFAP, host chicken, Nordic BioSite, diluted 1:500 | Cy2 donkey anti-chicken, Jackson, diluted 1:500 |

Electron microscopic immunogold cytochemistry

Tissue blocks of 1x1 mm from SNpc and parietal cortex were dissected out using a dissection microscope (Olympus SZX12, Tokyo, Japan). The tissue blocks were subjected to freeze substitution procedure as previously described (van Lookeren Campagne et al. 1991) for the untreated animals and for the MPTP and saline treated animals. In brief, the tissue blocks were cryo-protected in glycerol and rapidly frozen in liquid propane at -170ºC. The frozen tissue was immersed into anhydrous methanol containing 1.5% uranyl acetate at 90ºC in an automatic freeze substitution unit (EMAFS, Leica, Vienna, Austria), infiltrated with Lowicryl HM20 Resin (Lowy, Waldkraiburg, Germany) at -30ºC and polymerized by ultraviolet light. Ultrathin sectioning and immunogold labeling were performed as described previously (Hoddevik et al. 2016). Briefly, the blocks were cut into ultrathin sections of 90-100 nm using an ultramicrotome (Leica EM UC6, Vienna, Austria), transferred to mesh grids and incubated in drops of Tris-buffered saline (HCl 0.3%, NaCl 0.01%) with 0.1% triton (TBST) and 50 mM glycine for 10 minutes, washed in double distilled water and then incubated for 10

minutes in TBST containing 2% w/v human serum albumin (HSA). The grids were then incubated in a solution of 2% w/v HSA in TBST and the primary antibody (table 1) over night at room temperature. The labeling was visualized with a secondary antibody coupled to 15 nm colloidal gold particles (table 1) diluted in 1:20 TBST with 2% w/v HSA and polyethylene glycol. The sections were contrasted with 1% uranyl acetate and 0.3% lead citrate for 1.5 min and rinsed in double distilled water in between. The sections were finally examined with an electron microscope (Tecnai 12, FEI Company, Eindhoven, Netherlands). Random microvessels (n=25) were selected from each section at low magnification and one electron microscopic image of the perivascular endfoot was acquired per capillary. For the analysis of the non-endfoot AQP4 immunogold labeling, 20 electron micrographs of the neuropil were randomly obtained throughout each section at 20500x magnification. The analyzer was blind to treatment and area.

**Quantification and statistical analysis**

Postembedding immunogold microscopy and quantification of AQP4 labeling

For the quantification of the AQP4 distribution in untreated and MPTP/saline treated SNpc and parietal cortex, images from capillaries were selected in a blinded manner from each section (one section for each animal) and quantified with an image analysis program, analySIS Pro version 3.2 (Soft Imaging System GmbH, Munster, Germany) for the untreated sections and analySIS IMGAP version Beta cell^p (Soft Imaging Systems GmbH, Munster, Germany) for the MPTP/saline treated sections. Larger vessels and distorted or mechanically damaged basal lamina were excluded, as well as non-neuropil components such as neurons and vessels for the neuropil electron micrographs. Membrane segments of interest and membrane curves were drawn in the overlay interactively; the membrane segment of the astrocyte endfoot facing the capillary lumen was called *ad*luminal and the membrane segment facing neuropil was called *ab*luminal. Both membrane segments were analyzed in the MPTP/saline treated sections and only the adluminal segment was analyzed in the untreated sections. Gold particles near each membrane curve were detected semi-automatically, and the distance between each particle and its membrane curve was calculated by the program. Particles localized within 23.5 nm from their membrane curve (Amiry-Moghaddam and Ottersen 2013) were included in the calculation of the number of particles per µm of membrane (linear particle density). In the neuropil area, gold particles per $\mu m^2$ were

calculated by the program after drawing an area of interest in the overlay for each section. The non-endfoot astrocyte processes in the neuropil were called non-end. Groups were analyzed statistically by Student's *t*-test (two-tailed) using SPSS version 18.0 for the untreated sections and version 22.0 for the MPTP/saline treated sections. The significance level was set to 0.05.

## RESULTS

### AQP4 in normal, untreated animals

Immunofluorescence analysis demonstrated highly polarized expression of AQP4 around blood vessels in SNpc (Fig. 1A-D) and neocortex (Fig. 1E-H). In neocortex, AQP4 is scarce in the neuropil and around profiles positive for the neuronal marker TuJ1 (Fig. 1E-H).

In the SNpc, AQP4 is abundantly expressed with a particularly pronounced labeling in perivascular astrocyte processes. AQP4 immunolabeling is also found in non-endfoot membranes in the neuropil. A similar pattern occurs in the pars reticulata, where the density of TH positive cells is lower and the density of GFAP positive cells is higher than in the pars compacta (Fig. 1A-D).

In line with the immunofluorescence labeling, electron micrograph images demonstrated a particularly dense immunolabeling of AQP4 in the SN (Fig. 2A) compared to neocortex (Fig. 2B). AQP4 immunogold particles were concentrated in perivascular endfoot membranes, and were also numerous in fine astrocytic processes in the neuropil. Compared to the neocortex, the SN showed stronger AQP4 immunolabeling both perivascularly (Fig. 2C) and in neuropil (Fig. 2D). In the SN, perivascular labeling was 70% higher than in the neocortex, with a mean linear density of 28.4 ± 1.0 gold particles/µm compared to 16.8 ± 0.7 gold particles/µm in the neocortex ($p<0.001$). Non-endfoot labeling was measured as areal density of gold particles in randomly selected images from neuropil. In the SN, density of AQP4 immunogold particles was 12.7 ± 1.6 gold particles/$\mu m^2$, compared to 5.5 ± 0.5 gold particles/$\mu m^2$ in the neocortex ($p<0.001$) (values are mean ± SEM). These results complement and extend the immunofluorescence data.

**AQP4 in MPTP-treated animals**

MPTP induces dopaminergic cell death, as seen by loss of tyrosine hydroxylase (TH) positive cells. The method of quantification and the level of degeneration of TH positive neurons in the SNpc in the MPTP treated mice were previously described (Puchades et al. 2013). MPTP treatment led to a 42% reduction in the density of TH positive cell bodies (Puchades et al. 2013). Immunofluorescence analysis of SN revealed that MPTP injections led to strong upregulation of AQP4, both perivascularly and in non-endfoot membranes (Fig. 3A, B). Upregulation of glial fibrillary acidic protein (GFAP) was also observed, indicating reactive astrogliosis (Fig. 3C-D). This is consistent with previous findings (Puchades et al. 2013). No change was found in control animals injected with saline (Fig. 3E-H).

In accordance with the immunofluorescence labeling, immunoelectron microscopy of SNpc of MPTP treated animals showed an increased expression of AQP4 both in the perivascular endfoot membranes and in the non-endfoot membranes in the neuropil (Fig. 4).

The quantitative analysis of MPTP treated animals revealed in SNpc a significantly higher expression of AQP4 in the *ad*luminal as well as the *ab*luminal membranes of perivascular endfeet. The adluminal labeling was 30% higher in MPTP treated animals than in saline controls, with a mean linear density of 30.3 ± 1.21 gold particles/µm and 23.5 ± 1.05 ($p< 0.05$), respectively (Fig. 5A). The abluminal labeling was 34% higher in the MPTP treated animals than in the saline controls with a mean linear density of 15.3 ± 1.02 gold particles/ µm compared to 11.4 ± 0.71 in the saline controls ($p < 0.01$) (Fig. 5A). In line with the immunofluorescence data, the quantitative immunogold analysis revealed an increased expression of AQP4 in the non-endfoot astrocytic membranes following MPTP injections. The neuropil labeling was 21% higher in the animals treated with MPTP, with a mean linear density of 6.3 ± 0.36 gold particles / $\mu m^2$ compared to 5.2 ± 0.28 ($p = 0.019$) (Fig. 5B).

Administration of MPTP also caused a modest increase in perivascular AQP4 immunolabeling in the neocortex. The changes were restricted to the adluminal membrane domains (Fig. 5C).

## DISCUSSION

Information is scant on the microscopic and fine structural localization of AQP4 in the SN. This void must be filled, as aquaporins and water homeostasis have become increasingly relevant in the context of PD. Notably, experimental data suggest that the toxin susceptibility of dopaminergic neurons depends on the level of AQP4 expression (Zhang et al. 2016) and a recent report based on a diffusion MRI technique has shown increased levels of free water in SNpc of patients with PD (Ofori et al. 2015b). There was a positive correlation between Montreal Cognitive Assessment scores and free water values in SNpc (Ofori et al. 2015a; Ofori et al. 2015b).

Our study is the first detailed study of AQP4 in the SN and shows that the perivascular AQP4 pool – which is relatively large even in normal animals – is further increased after treatment with MPTP. This suggests an involvement of AQP4 in PD and may explain why PD patients exhibit water accumulation in SN. These data contrast with findings in Alzheimer's disease, stroke and epilepsy, in which the perivascular AQP4 pool is reduced (Yang et al. 2011; Frydenlund et al. 2006; Alvestad et al. 2013). After experimental stroke, the endfoot pool of AQP4 is unaltered or increased in the initial phase, but then decreases sharply to very low levels at ~24 h of the ischemic episode (Frydenlund et al. 2006; De Castro Ribeiro et al. 2006)

Our results show that AQP4 is more plentiful in the SN than in the neocortex, both in endfoot membranes encompassing microvessels and in non-endfoot astrocytic membranes in the neuropil. This high density of AQP4 was further increased following injections of MPTP. Our conclusions were based on a postembedding immunogold technique that has been modified so as to enable a precise localization and quantification of membrane-bound AQP4 (Amiry-Moghaddam and Ottersen 2013; Takumi et al. 1998).

Attempts to identify mechanisms underlying the selective vulnerability of dopaminergic cells in the SNpc have focused primarily on the neurons. Although astrocytes are known to be essential in maintenance of homeostatic processes and neuronal function, little is known about their roles in the pathophysiology of PD. The density of astrocytes in the SNpc is low compared to that in other regions (Ji et al. 2008). As astrocytes release a variety of growth factors under normal conditions (Swanson et al. 2002), one could ask if this low density of astrocytes in SNpc would contribute to the susceptibility of local dopaminergic neurons. Another question is whether nigral astrocytes differ from other astrocytes when it comes to

their roles in maintaining key homeostatic functions. The present analysis of AQP4 was prompted by this question.

To shed light on the potential role of astrocytes and AQP4 in the pathophysiology of PD, we studied AQP4 expression pattern in an acute MPTP mouse model of PD. MPTP induces a parkinsonian syndrome by inactivating complex I of the electron transfer chain (Nicklas et al. 1987). It has also been reported that MPTP treatment leads to astrogliosis in SNpc, as well as in striatum (Puchades et al. 2013). In this respect, it should be noted that the death of dopamine neurons increases between day 1 and 4 after MPTP treatment, and the number of degenerated neurons is thereafter stable for at least one month (Jackson-Lewis et al. 1995). Astrogliosis follows a similar time course; starting at day1 and increasing till day 7 after MPTP, when it reaches a plateau where the number of reactive astrocytes is more or less stable for one month (Hou et al. 2017).

Our study revealed a general upregulation of AQP4 expression in SNpc in the animals treated with MPTP. The high resolution immunogold analysis allowed us to distinguish between different subcellular AQP4 pools and identified a pronounced increase in the density of AQP4 in the astrocytic endfoot membranes that enwrap capillaries and microvessels. This perivascular pool of AQP4 is the one that is directly engaged in water exchange between blood and brain and that controls the influx of water in pathological conditions such as stroke and hyponatremic brain edema (Amiry-Moghaddam et al. 2003; Amiry-Moghaddam et al. 2004). An increased perivascular pool of AQP4 would make the SN more prone to water accumulation – thus providing a possible mechanistic explanation for the abnormal water contents seen in SN of patients with PD (Ofori et al. 2015a).

The present data call for further studies to disentangle the possible coupling between astrocytic dysfunction and the propensity for developing PD – be it in its idiopathic form or in response to known parkinsonogenic drugs. A number of neurological conditions have been associated with perturbations of water and ion homeostasis, and mislocalization of astrocytic AQP4 occurs in human temporal lobe epilepsy as well as in animal models of stroke and Alzheimer's disease (Eid et al. 2005; Yang et al. 2011). In the kainate model of epilepsy, mislocalization of AQP4 was found to precede the development of overt seizures, suggesting a role in pathogenesis (Alvestad et al. 2013). In terms of AQP4 mislocalization, PD differs

from the above conditions in showing an increase, rather than a decrease, of AQP4 in perivascular membranes.

It should be emphasized that the increase in the expression of AQP4 which is observed in our study can not be explained solely by gliosis. Indeed, gliosis is observed in the sclerotic hippocampus of patients with mesial temporal lobe epilepsy and in the mouse models of Alzheimer's disease. In both conditions gliosis is associated with a loss rather than an increase of endfoot AQP4 (Eid et al. 2005; Yang et al. 2011). Also in a model of cerebral malaria there is an overall decrease in AQP4 expression, despite extensive gliosis (Promeneur et al. 2013). Further studies are needed to unravel the mechanistic link between AQP4 expression and proneness to PD and – in a longer time perspective - to ascertain whether astrocytes could serve as targets of new therapies.

*Acknowledgements:* The authors would like to thank Bjørg Riber, Karen Marie Gujord, Jorunn Knutsen and Bashir Hakim for technical assistance and Gunnar Lothe for graphics. This study was supported by M.D. Ph.D Curriculum of the medical faculty at the University of Oslo

## References

Alvestad S, Hammer J, Hoddevik EH, Skare Ø, Sonnewald U, Amiry-Moghaddam M, Ottersen OP (2013) Mislocalization of AQP4 precedes chronic seizures in the kainate model of temporal lobe epilepsy. Epilepsy research 105 (1-2):30-41. doi:10.1016/j.eplepsyres.2013.01.006

Amiry-Moghaddam M, Otsuka T, Hurn PD, Traystman RJ, Haug F-M, Froehner SC, Adams ME, Neely JD, Agre P, Ottersen OP, Bhardwaj A (2003) An alpha-syntrophin-dependent pool of AQP4 in astroglial end-feet confers bidirectional water flow between blood and brain. Proceedings of the National Academy of Sciences of the United States of America 100 (4):2106

Amiry-Moghaddam M, Ottersen OP (2003) The molecular basis of water transport in the brain. Nature Reviews Neuroscience 4 (12):991. doi:10.1038/nrn1252

Amiry-Moghaddam M, Ottersen OP (2013) Immunogold cytochemistry in neuroscience. Nature neuroscience 16 (7):798-804. doi:10.1038/nn.3418

Amiry-Moghaddam M, Xue R, Haug F-M, Neely JD, Bhardwaj A, Agre P, Adams ME, Froehner SC, Mori S, Ottersen OP (2004) Alpha-syntrophin deletion removes the perivascular but not endothelial pool of aquaporin-4 at the blood-brain barrier and delays the development of brain edema in an experimental model of acute hyponatremia. FASEB journal : official publication of the Federation of American Societies for Experimental Biology 18 (3):542

De Castro Ribeiro M, Hirt L, Bogousslavsky J, Regli L, Badaut J (2006) Time course of aquaporin expression after transient focal cerebral ischemia in mice. Journal of neuroscience research 83 (7):1231-1240. doi:10.1002/jnr.20819

Eid T, Tih-Shih WL, Marion JT, Mahmood A-M, Lars PB, Dennis DS, Peter A, Ole PO, Nihal CdL (2005) Loss of perivascular aquaporin 4 may underlie deficient water and K+ homeostasis in the human epileptogenic hippocampus. Proceedings of the National Academy of Sciences of the United States of America 102 (4):1193. doi:10.1073/pnas.0409308102

Eilert-Olsen M, Haj-Yasein NN, Vindedal GF, Enger R, Gundersen GA, Hoddevik EH, Petersen PH, Haug F-MS, Skare Ø, Adams ME, Froehner SC, Burkhardt JM, Thoren AE, Nagelhus EA (2012)

Deletion of aquaporin-4 changes the perivascular glial protein scaffold without disrupting the brain endothelial barrier. Glia 60 (3):432. doi:10.1002/glia.22277
Fan Y, Kong H, Shi X, Sun X, Ding J, Wu J, Hu G (2008) Hypersensitivity of aquaporin 4-deficient mice to 1-methyl-4-phenyl-1,2,3,6-tetrahydropyrindine and astrocytic modulation. Neurobiology of Aging 29 (8):1226-1236. doi:10.1016/j.neurobiolaging.2007.02.015
Frydenlund DS, Bhardwaj A, Otsuka T, Mylonakou MN, Yasumura T, Davidson KGV, Zeynalov E, Skare Ø, Laake P, Haug F-M, Rash JE, Agre P, Ottersen OP, Amiry-Moghaddam M (2006) Temporary Loss of Perivascular Aquaporin-4 in Neocortex after Transient Middle Cerebral Artery Occlusion in Mice. Proceedings of the National Academy of Sciences of the United States of America 103 (36):13532-13536. doi:www.pnas.org/cig/doi/10.1073/pnas.0605796103
Hirsch EC, Jenner P, Przedborski S (2013) Pathogenesis of Parkinson's Disease. Mov. Disord., vol 28. doi:10.1002/mds.25032
Hoddevik EH, Khan FH, Rahmani S, Ottersen OP, Boldt HB, Amiry-Moghaddam M (2016) Factors determining the density of AQP4 water channel molecules at the brain–blood interface. Brain Structure and Function:1-14. doi:10.1007/s00429-016-1305-y
Hou L, Zhou X, Zhang C, Wang K, Liu X, Che Y, Sun F, Li H, Wang Q, Zhang D, Hong J-S (2017) NADPH oxidase-derived H2O2 mediates the regulatory effects of microglia on astrogliosis in experimental models of Parkinson's disease. Redox Biology. doi:10.1016/j.redox.2017.02.016
Jackson-Lewis V, Jakowec M, Burke RE, Przedborski S (1995) Time course and morphology of dopaminergic neuronal death caused by the neurotoxin 1-methyl-4-phenyl-1,2,3,6-tetrahydropyridine. Neurodegeneration 4 (3):257-269. doi:10.1016/1055-8330(95)90015-2
Ji K, Eu M, Kang S, Gwag B, Jou I, Joe E (2008) Differential neutrophil infiltration contributes to regional differences in brain inflammation in the substantia nigra pars compacta and cortex. Glia 56 (10):1039-1047. doi:10.1002/glia.20677
Mena MA, García De Yébenes J (2008) Glial cells as players in parkinsonism: The "good," the "bad," and the "mysterious" glia. The Neuroscientist : a review journal bringing neurobiology, neurology and psychiatry 14 (6):544-560. doi:10.1177/1073858408322839
Nagelhus EA, Horio Y, Inanobe A, Fujita A, Haug Fm, Nielsen S, Kurachi Y, Ottersen OP (1999) Immunogold evidence suggests that coupling of K + siphoning and water transport in rat retinal Müller cells is mediated by a coenrichment of Kir4.1 and AQP4 in specific membrane domains. Glia 26 (1):47-54. doi:10.1002/(sici)1098-1136(199903)26:1<47::aid-glia5>3.0.co;2-5
Nicklas WJ, Youngster SK, Kindt MV, Heikkila RE (1987) MPTP, MPP+ and mitochondrial function. Life sciences 40 (8):721
Nielsen S, Nagelhus EA, Amiry-Moghaddam M, Bourque C, Agre P, Ottersen OP (1997) Specialized membrane domains for water transport in glial cells: high-resolution immunogold cytochemistry of aquaporin-4 in rat brain. The Journal of neuroscience : the official journal of the Society for Neuroscience 17 (1):171
Ofori E, Pasternak O, Planetta PJ, Burciu R, Snyder A, Febo M, Golde TE, Okun MS, Vaillancourt DE (2015a) Increased free water in the substantia nigra of Parkinson's disease: a single-site and multi-site study. Neurobiology of Aging 36 (2):1097-1104. doi:10.1016/j.neurobiolaging.2014.10.029
Ofori E, Pasternak O, Planetta PJ, Li H, Burciu RG, Snyder AF, Lai S, Okun MS, Vaillancourt DE (2015b) Longitudinal changes in free-water within the substantia nigra of Parkinson's disease. Brain 138 (8):2322-2331. doi:10.1093/brain/awv136
Promeneur D, Lunde LK, Amiry-Moghaddam M, Agre P (2013) Protective role of brain water channel AQP4 in murine cerebral malaria. Proceedings of the National Academy of Sciences of the United States of America 110 (3):1035-1040. doi:10.1073/pnas.1220566110
Puchades M, Sogn CJ, Maehlen J, Bergersen LH, Gundersen V (2013) Unaltered lactate and glucose transporter levels in the MPTP mouse model of Parkinson's disease. Journal of Parkinson's disease 3 (3):371. doi:10.3233/jpd-130190

Rash JE, Yasumura T, Hudson CS, Agre P, Nielsen S (1998) Direct immunogold labeling of aquaporin-4 in square arrays of astrocyte and ependymocyte plasma membranes in rat brain and spinal cord. Proceedings of the National Academy of Sciences of the United States of America 95 (20):11981-11986

Saadoun S, Papadopoulos MC, Hara-Chikuma M, Verkman AS (2005) Impairment of angiogenesis and cell migration by targeted aquaporin-1 gene disruption. Nature 434 (7034):786-792. doi:10.1038/nature03460

Sun H, Liang R, Yang B, Zhou Y, Liu M, Fang F, Ding J, Fan Y, Hu G (2016) Aquaporin-4 mediates communication between astrocyte and microglia: Implications of neuroinflammation in experimental Parkinson's disease. Neuroscience 317:65-75. doi:10.1016/j.neuroscience.2016.01.003

Swanson RA, Ying W, Alano CC, Chen Y (2002) PARP‐1 activation causes mitochondrial dysfunction. Journal of neurochemistry 81:108-111. doi:10.1046/j.1471-4159.81.s1.42_5.x

Takumi Y, Nagelhus E, Eidet J, Matsubara A, Usami S, Shinkawa H, Nielsen S, Ottersen O (1998) Select types of supporting cell in the inner ear express aquaporin-4 water channel protein. Eur J Neurosci 10 (12):3584-3595

Thrane AS, Rappold PM, Fujita T, Torres A, Bekar LK, Takano T, Peng W, Wang F, Rangroo Thrane V, Enger R, Haj-Yasein NN, Skare Ø, Holen T, Klungland A, Ottersen OP, Nedergaard M, Nagelhus EA (2011) Critical role of aquaporin-4 (AQP4) in astrocytic Ca2+ signaling events elicited by cerebral edema. Proceedings of the National Academy of Sciences of the United States of America 108 (2):846. doi:10.1073/pnas.1015217108

van Lookeren Campagne M, Oestreicher AB, van Der Krift TP, Gispen WH, Verkleij AJ (1991) Freeze-substitution and Lowicryl HM20 embedding of fixed rat brain: suitability for immunogold ultrastructural localization of neural antigens. The journal of histochemistry and cytochemistry : official journal of the Histochemistry Society 39 (9):1267

Vernice J-L, Serge P (2007) Protocol for the MPTP mouse model of Parkinson's disease. Nature Protocols 2 (1):141. doi:10.1038/nprot.2006.342

Yang J, Lunde L, Nuntagij P, Oguchi T, Camassa L, Nilsson LNG, Lannfelt L, Xu Y, Amiry-Moghaddam M, Ottersen O, Torp R (2011) Loss of Astrocyte Polarization in the Tg-ArcSwe Mouse Model of Alzheimer's Disease. J Alzheimers Dis 27 (4):711-722. doi:10.3233/jad-2011-110725

Zhang J, Yang B, Sun H, Zhou Y, Liu M, Ding J, Fang F, Fan Y, Hu G (2016) Aquaporin-4 deficiency diminishes the differential degeneration of midbrain dopaminergic neurons in experimental Parkinson's disease. Neuroscience Letters 614:7-15. doi:10.1016/j.neulet.2015.12.057

## Fig. legends

Fig. 1: Distribution of AQP4 in substantia nigra (SN; A-D) and cerebral cortex (CX; E-H). Strong AQP4 immunofluorescent staining (red) is present in the astrocyte processes in neuropil (asterisk) and around blood vessels (white arrows) in SN (A). In the cortex, AQP4 expression is restricted to astrocytic endfeet facing blood vessels and the pial surface (white arrow head) (E). Tyrosine hydroxylase (TH; green) is used as a marker for dopaminergic neurons in SNpc (B), and tubulin class III (TuJ1; green) is used as a general neuronal marker in CX (F). Astrocytic processes with endfoot membranes abutting microvessels and the pial surface (white arrow head, G) are visualized by GFAP (orange). Merged images show co-

localization of AQP4 with GFAP in both SN (D) and CX (H). SNpc; Substantia nigra pars compacta, and SNpr; Substantia nigra pars reticulata. n=5, scale bar: 50 µm.

Fig.: 2: Immunogold labeling and quantitative analysis of AQP4-labeling in substantia nigra (SN) and neocortex (CX) in untreated animals. The AQP4 immunogold labeling at the perivascular astrocyte membrane domains (arrow) is stronger in the SN (A) than in the CX (B). Quantitative analysis of the perivascular immunogold labeling shows a significantly higher mean linear density of gold particles in the SN, compared to the CX (*** $p<0.001$) (C). Non-endfoot membranes show significantly higher density of AQP4 immunogold particles in the SN compared to CX (*** $p<0.001$) (D). n=3, scale bar: 1 µm.

Fig. 3: Expression of AQP4, TH positive cells and GFAP in SN in the MPTP mouse model of PD (A-D) compared to the saline control (E-H). Subcutaneous injections of MPTP resulted in strong upregulation of AQP4 (red) in the SN, both perivascularly (white arrow) and in non-endfoot (asterisk) membranes (A). Further, the toxin induced dopaminergic cell death, as judged by loss of tyrosine hydroxylase (TH) positive cells (green, B). Upregulation of glial fibrillary acidic protein (GFAP; orange) was also observed, indicating astrogliosis (C, D). This reaction was not seen in control animals injected with saline (G, H). MPTP, n= 4; saline, n=3. Scale bar: 50 µm.

Fig. 4: Immunogold labeling of AQP4 in SN in animals exposed to MPTP (A, B) and saline injections (C, D). Electron micrograph imaging showed increased expression of AQP4 labeling in astrocytic perivascular endfoot membranes (A), both in the adluminal (black arrow) and in the abluminal (black arrow head) membrane, as well as in the astrocytic non-endfoot membranes in the neuropil (B, black arrow) compared to saline controls (C, D). L = lumen, E = endothelial cell. n= 5 for each experimental group, scale bar: 1 µm.

Fig. 5: Quantitative immunogold analysis of AQP4 in the SN and CX of animals injected with MPTP (n= 5) compared to animals injected with saline (n= 5; A-C). Quantitative analysis of the immunogold labeling at the perivascular astrocytic endfoot membrane domains in SN revealed a significantly higher linear density of AQP4 labeling in both the adluminal (* $p<0.05$) and abluminal (** $p<0.01$) membrane domains of the MPTP treated animals compared to the saline controls (A). The AQP4 immunogold labeling of the non-endfoot astrocyte processes in the SN is significantly higher in the MPTP treated mice compared to the saline controls (B, * $p<0.05$). Immunogold labeling of AQP4 in the CX shows a small but

significant increase in the perivascular astrocytic adluminal membrane domains (* p=0.041). No significant alteration in the AQP4 expression was detected in the astrocytic abluminal membrane domains (C).

**Figure 1**

**Click here to download high resolution image**

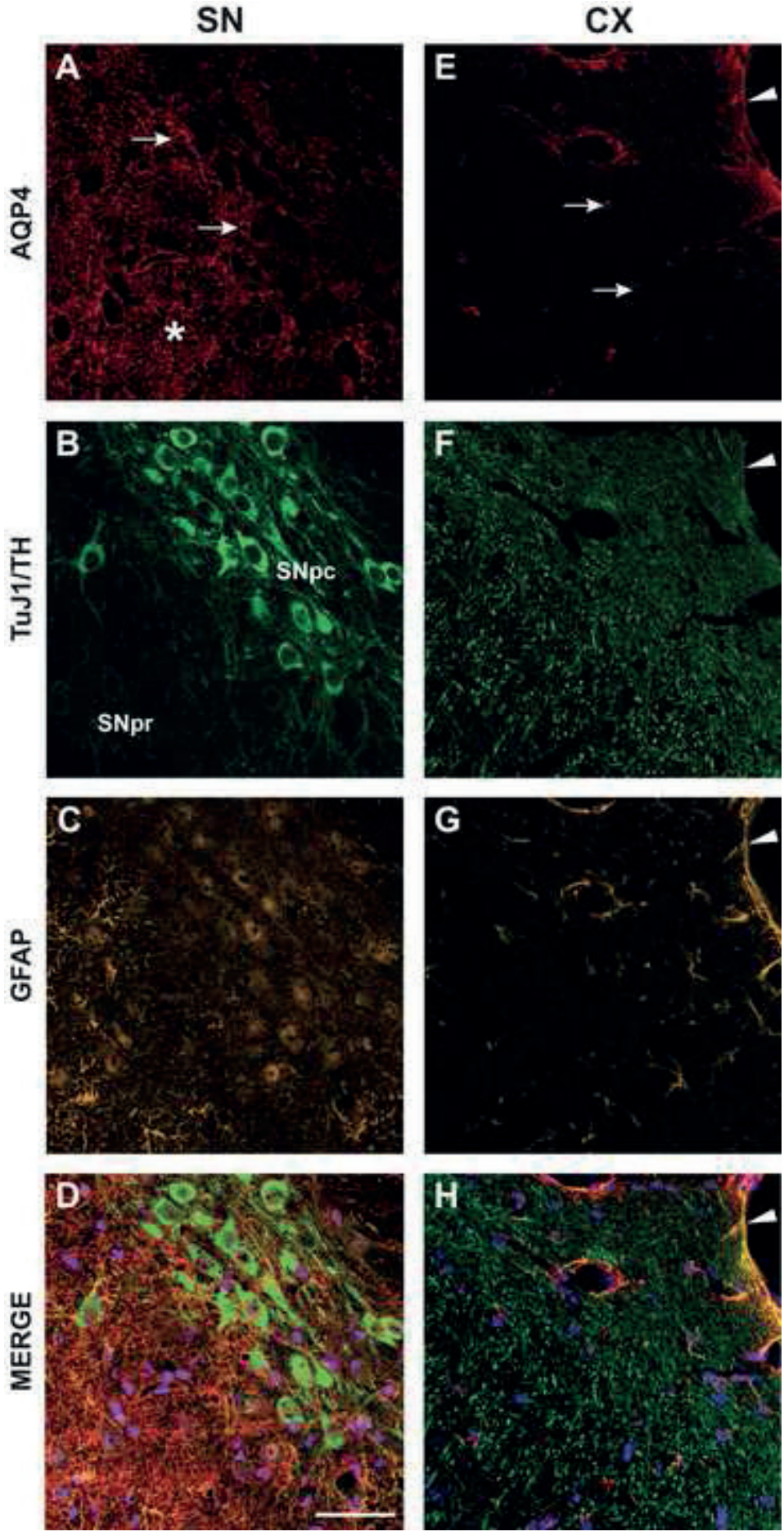

**Figure 2**
**Click here to download high resolution image**

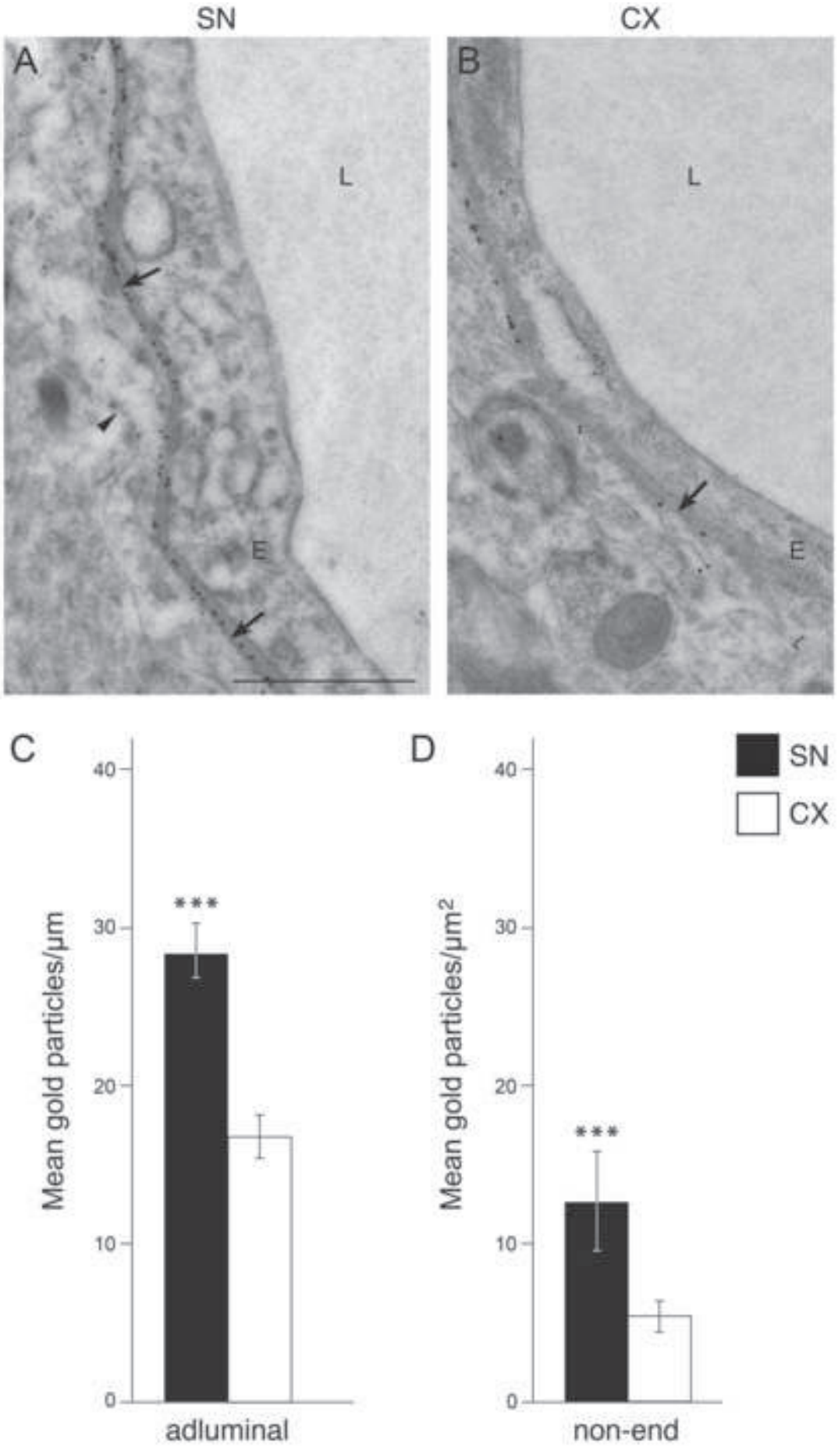

**Figure 3**

**Click here to download high resolution image**

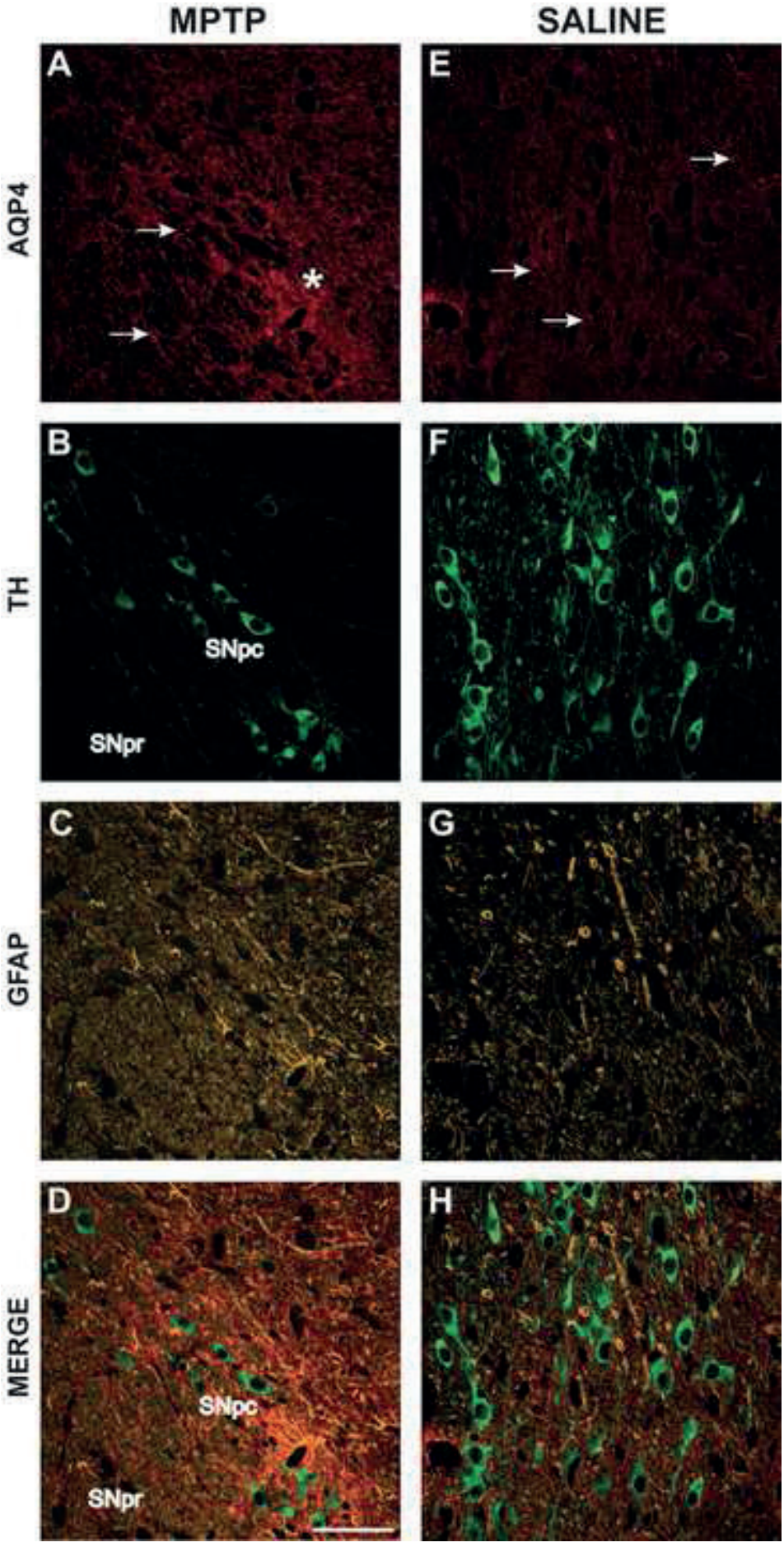

**Figure 4**

**Click here to download high resolution image**

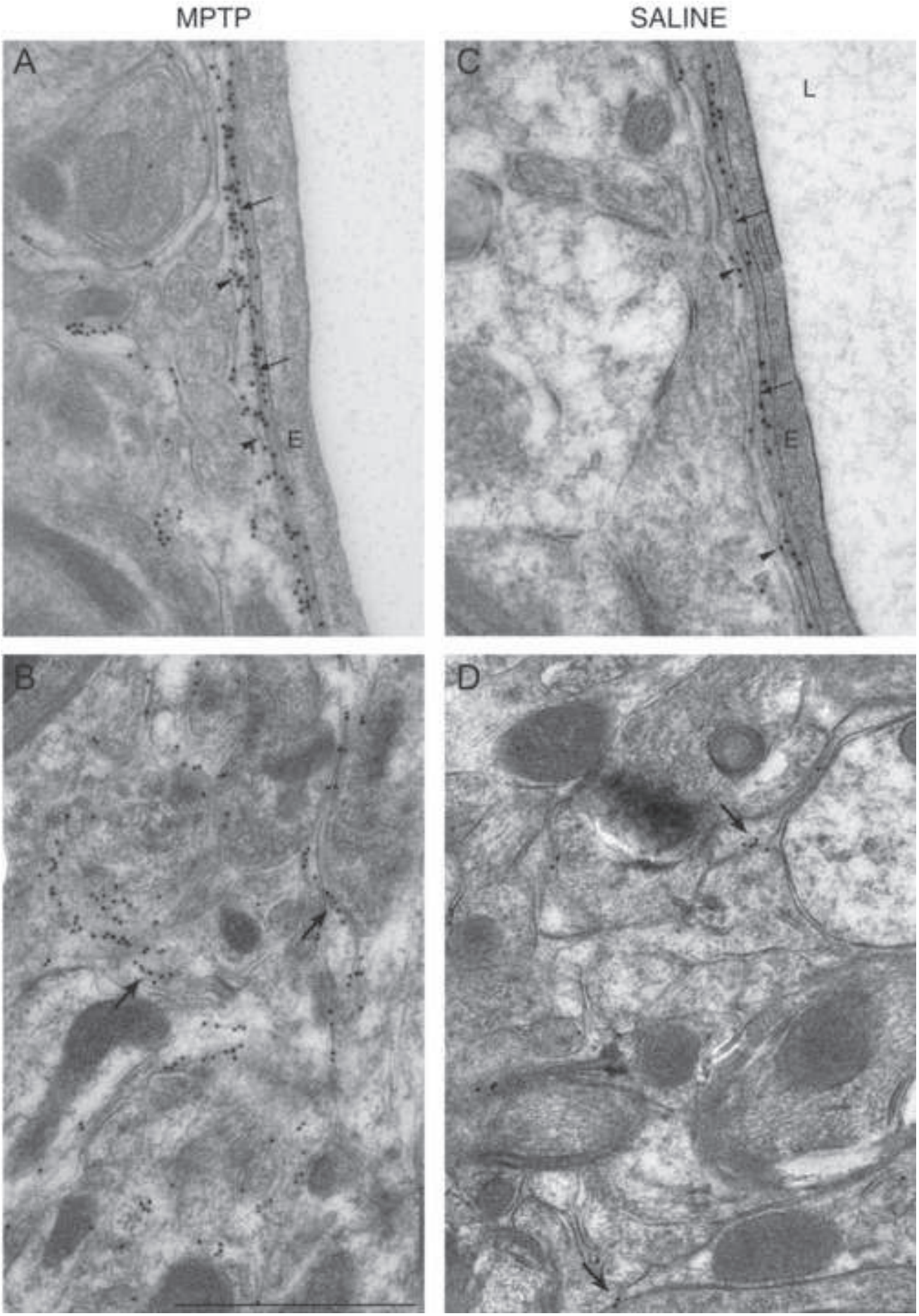

**Figure 5**
**Click here to download high resolution image**